Deep Learning Imaging through Specialty Multi-mode Fibers

Jian Zhao,[1,2,*] Shengli Fan,[2] Jose Enrique Antonio-Lopez,[2] and Axel Schülzgen[2]
[1] *Boston University, Photonics Center, Boston, MA 02215, USA*
[2] *CREOL, College of Optics and Photonics, University of Central Florida, Orlando, FL 32816, USA*
**Corresponding author: JianZHAO@knights.ucf.edu*

Abstract: We demonstrate a cost-effective, highly accurate, and fast-speed cell sensing system enabled by the combination of the disordered optical fiber and the deep-learning classifier. It is compatible with both coherent and incoherent illumination.
OCIS codes: (060.2310) Fiber Optics; (060.2350) Fiber optics imaging; (060.4005) Microstructured fibers;

1. Introduction

In medical histology, it is crucial for a pathologist to identify and classify the diseased tissue accurately. The conventional histopathological examination requires the preparation of tissue sample slides which involves complicated surgical tissue-removal and chemical tissue-fixation procedures [1]. The subsequent diagnosis heavily relies on expensive bench-top microscopy and the visual inspection by a trained pathologist. This conventional method results in time-consuming, high-cost examinations and surgical trauma to patients. Especially, it is hard to achieve real-time *in vivo* examination of the diseased tissue with high accuracy. One potential solution to improve such identification and classification procedures is to combine a fiber-optic system (FOS) with deep learning algorithms. It is well known that the FOS could penetrate deep into tissues or hollow organs to collect scattered light in a minimally invasive way, which is inaccessible for conventional instruments [2]. By processing fiber-delivered optical information with the latest deep-learning algorithms, FOS could work as a cost-effective and high-speed *in vivo* histopathological examination tool with high accuracy and minimized damage to patients. Although many different types of optical fibers, including conventional multimode fibers and multicore fibers, can be utilized as the optical data transmission media, FOSs based on these conventional optical fibers face severe challenges including extreme bending and thermal sensitivity, low mode density, incompatibility with incoherent broadband illumination and high cost [2-4]. In contrast to conventional multimode and multicore fibers, recently developed glass-air Anderson localizing optical fibers (GALOFs) are becoming a promising alternative since they provide a high density, multichannel optical transmission system and GALOF-based FOSs have demonstrated superior performance that can overcome the abovementioned limitations [5-8]. The GALOF is a highly multimode system with the majority of the localized modes showing single-mode properties, such as bending independence, diffraction-limited beam quality, and high spatial coherence. Meanwhile, the mode density can be as high as ~10 modes per μm^2 and the localization size does not depend on the wavelength. Because of these unique properties, GALOFs provide robust and high-quality optical information transfer channels that are also compatible with broadband illumination. Here, we present a deep-learning-based GALOF FOS that collects and transmits light from various samples and demonstrate fast and accurate classification using either coherent or incoherent illumination.

2. Experiment and results

The schematic of the experimental setup and the architecture of the deep convolutional neural network classification model (DCNN-C) are shown in Fig. 1. The GALOF used in this work has an inner diameter of ~278 μm with an air-hole-filling fraction of 28.5 %. An SEM image of the cross-section structure is also shown in Fig. 1. Two separate experiments are performed. In the first experiment, we couple images of the Modified National Institute of Standards and Technology (MNIST) database of handwritten numbers into the GALOF input facet under continuous wave laser illumination (~405 nm wavelength). MNIST images are transmitted through ~80 cm of GALOF and recorded by the CCD camera (Manta G-145B). The MNIST images are 8-bit gray-scale intensity images generated by a spatial light modulator located between two linear polarizers. We use 5000 MNIST images as the training data and another 1000 images as the test data. The images in the test dataset never appear in the training dataset. The collected images are cropped to a pixel size of 512×512. Each image in the training dataset is labelled with the corresponding integer ground-truth values ranging from 0 to 9. In the second experiment, we couple the images of three different cell samples, which are stained and fixed on glass slides, into the GALOF input facet under incoherent broadband LED illumination (center wavelength ~460 nm). The three different cell samples are bird blood cells, human red blood cells, and cancerous human stomach cells, respectively. The experimental procedure is similar to the first experiment. However, here we use 15000 images as the training dataset and 1500 images as the

test dataset. The images of three different cell samples are labeled with the corresponding integer ground-truth values ranging from 0 to 2.

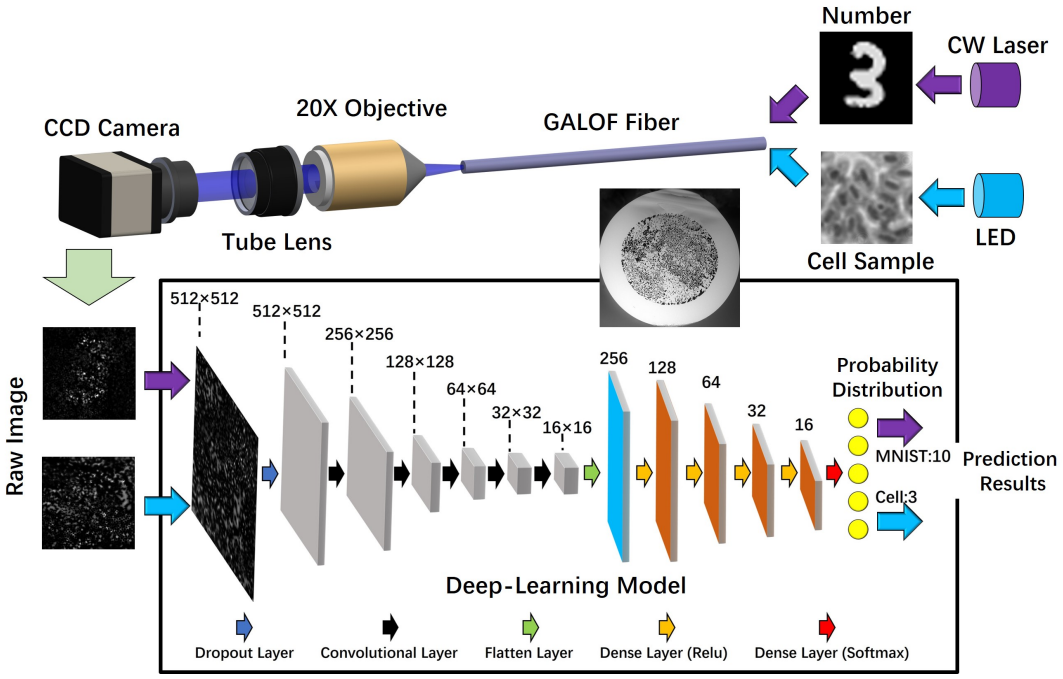

Fig. 1. Experimental setup and schematic of the DCNN-C architecture.

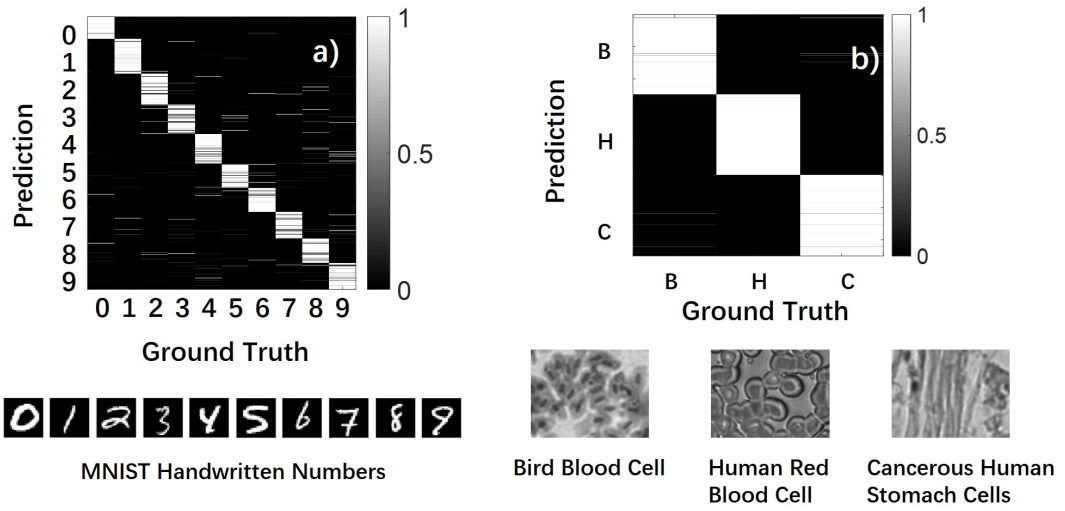

Fig. 2. Confusion matrices of DCNN-C prediction. a) Results for MNIST images. The average probability of an accurate prediction is ~90.0%. b) Results for cell images. The average probabilities of accurate predictions are 99.4%, 99.8% and 98.9% for bird blood cells, human red blood cells, and cancerous human stomach cells, respectively. (B: bird blood cells, H: human red blood cells, C: cancerous human stomach cells)

The architecture of the DCNN-C is shown in Fig. 1. The cropped raw image is first going through a dropout layer and then it is down-sampled by five convolutional neural network blocks to extract high-dimensional image features. The flatten layer reshapes the image feature map to a one-dimensional array that is followed by another four dense layers all with Relu as the activation function. Finally, the output dense layer with the Softmax activation function generates the prediction probability distribution. Depending on the number of ground-truth values, the length of the output vector can be either 10 for MNIST images or 3 for cell images. The model is developed based on the Keras framework. The Adam optimizer is applied in the training process with a batch size of 64 and 100 epochs in total. The regularizer applied in the DCNN-C is defined by the L2 norm. The filter sizes are 11×11 and 3×3 for MNIST

images and cell images, respectively. The test time for classifying an individual raw input image is about 30 milliseconds. The training time is about 0.5 hours and 1.5 hours for MNIST images and cell images, respectively. We use a GeForce 2080 Ti GPU to perform the training and the test processes. The test classification results for MNIST images and cell images are given in Fig. 2 a) and b), respectively. Different gray values in the confusion matrices stand for different probabilities of accurate classification. The average probability for accurately predicting an MNIST handwritten number is about 90%. The average probability for accurately classifying the cell type is even higher, with 99.4%. 99.8% and 98.9% for bird blood cell, human red blood cell, and cancerous human stomach cell, respectively. These test results demonstrate, that the GALOF/DCNN-C system is able to provide very fast and accurate classification of various sample objects under both coherent and incoherent illumination.

3. Conclusion

In conclusion, a deep-learning and GALOF-based classification system that features simple configuration, fast speed, and high accuracy is demonstrated for the first time for both coherent and incoherent illumination. GALOF-based fiber-optic imaging and classification systems have great potential to perform *in vivo* and real-time histopathological examinations for clinical applications.

4. References

[1] P. Fioretto and M. Mauer, "Histopathology of Diabetic Nephropathy," Seminars in Nephrology **27**, 195-207 (2007).
[2] B. A. Flusberg, E. D. Cocker, W. Piyawattanametha, J. C. Jung, E. L. Cheung, and M. J. Schnitzer, "Fiber-optic fluorescence imaging," Nat Methods **2**, 941-950 (2005).
[3] J. M. Stone, H. A. C. Wood, K. Harrington, and T. A. Birks, "Low index contrast imaging fibers," Optics Letters **42**, 1484-1487 (2017).
[4] S. Ohayon, A. Caravaca-Aguirre, R. Piestun, and J. J. DiCarlo, "Minimally invasive multimode optical fiber microendoscope for deep brain fluorescence imaging," Biomed. Opt. Express **9**, 1492-1509 (2018).
[5] J. Zhao, J. E. A. Lopez, Z. Zhu, D. Zheng, S. Pang, R. A. Correa, and A. Schülzgen, "Image Transport Through Meter-Long Randomly Disordered Silica-Air Optical Fiber," Scientific Reports **8**, 3065 (2018).
[6] B. Abaie, M. Peysokhan, J. Zhao, J. E. Antonio-Lopez, R. Amezcua-Correa, A. Schülzgen, and A. Mafi, "Disorder-induced high-quality wavefront in an Anderson localizing optical fiber," Optica **5**, 984-987 (2018).
[7] J. Zhao, Y. Sun, Z. Zhu, J. E. Antonio-Lopez, R. A. Correa, S. Pang, and A. Schülzgen, "Deep Learning Imaging through Fully-Flexible Glass-Air Disordered Fiber," ACS Photonics **5**, 3930-3935 (2018).
[8] J. Zhao, M. Peysokhan, J. E. Antonio-Lopez, Y. Sun, B. Abaie, A. Mafi, R. Amezcua Correa, S. Pang, and A. Schülzgen, "A path to high-quality imaging through disordered optical fibers: a review," Appl. Opt. **58**, D50-D60 (2019).